TISSUE ENGINEERING: Part A
Volume 23, Numbers 23 and 24, 2017
© Mary Ann Liebert, Inc.
DOI: 10.1089/ten.tea.2017.0111

termis
Tissue Engineering
& Regenerative Medicine
International Society

SPECIAL FOCUS: STRATEGIC DIRECTIONS IN OSTEOINDUCTION AND BIOMIMETICS*

Calvarial Bone Regeneration Is Enhanced by Sequential Delivery of FGF-2 and BMP-2 from Layer-by-Layer Coatings with a Biomimetic Calcium Phosphate Barrier Layer

Gloria Gronowicz, PhD,[1] Emily Jacobs, PhD,[2] Tao Peng, MD, PhD,[2] Li Zhu, MD,[2] Marja Hurley, MD,[3] and Liisa T. Kuhn, PhD[2]

A drug delivery coating for synthetic bone grafts has been developed to provide sequential delivery of multiple osteoinductive factors to better mimic aspects of the natural regenerative process. The coating is composed of a biomimetic calcium phosphate (bCaP) layer that is applied to a synthetic bone graft and then covered with a poly-L-Lysine/poly-L-Glutamic acid polyelectrolyte multilayer (PEM) film. Bone morphogenetic protein-2 (BMP-2) was applied before the coating process directly on the synthetic bone graft and then, bCaP-PEM was deposited followed by adsorption of fibroblast growth factor-2 (FGF-2) into the PEM layer. Cells access the FGF-2 immediately, while the bCaP-PEM temporally delays the cell access to BMP-2. *In vitro* studies with cells derived from mouse calvarial bones demonstrated that Sca-1 and CD-166 positive osteoblast progenitor cells proliferated in response to media dosing with FGF-2. Coated scaffolds with BMP-2 and FGF-2 were implanted in mouse calvarial bone defects and harvested at 1 and 3 weeks. After 1 week *in vivo*, proliferation of cells, including Sca-1+ progenitors, was observed with low dose FGF-2 and BMP-2 compared to BMP-2 alone, indicating that *in vivo* delivery of FGF-2 activated a similar population of cells as shown by *in vitro* testing. At 3 weeks, FGF-2 and BMP-2 delivery increased bone formation more than BMP-2 alone, particularly in the center of the defect, confirming that the proliferation of the Sca-1 positive osteoprogenitors by FGF-2 was associated with increased bone healing. Areas of bone mineralization were positive for double fluorochrome labeling of calcium and alkaline phosphatase staining of osteoblasts, along with increased TRAP+ osteoclasts, demonstrating active bone formation distinct from the bone-like collagen/hydroxyapatite scaffold. In conclusion, the addition of a bCaP layer to PEM delayed access to BMP-2 and allowed the FGF-2 stimulated progenitors to populate the scaffold before differentiating in response to BMP-2, leading to improved bone defect healing.

Keywords: calcium phosphate, fibroblast growth factor-2, bone morphogenetic protein-2, bone tissue engineering, polyelectrolyte multilayer

Introduction

THE NATURAL PROCESSES of tissue development or tissue repair involve the sequential synthesis, secretion, and assembly of different matrix components, growth factors, and other proteins to guide cell migration, proliferation, differentiation, and eventually cell death. Combinations of growth factors that aid different steps of regeneration are thus anticipated to synergistically enhance tissue regeneration. Several different types of delivery systems for multiple growth factors have been developed as potential therapeutics for wound healing/infection, bone, cartilage, muscle, teeth, and cancer, and have shown some efficacy both *in vitro*[1–5] and *in vivo*[6–8]; however, their success has been limited.

For some combinations of molecules, solution spiking experiment has shown that there is a need for sequential, rather than codelivery of growth factors from biomaterials to avoid conflicting cell signals.[2] Many of the drug delivery systems developed thus far, including microspheres,[1] nanoparticles,[4] and hydrogels,[7] result in codelivery profiles when multiple biomolecules are delivered. Natural biological processes involve the temporal presentation of factors in a

Departments of [1]Surgery, [2]Biomedical Engineering, and [3]Medicine, University of Connecticut Health Center, Farmington, Connecticut.

*This article is part of a special focus issue on Strategic Directions in Osteoinduction and Biomimetics.

sequential and carefully controlled manner by cells. Thus, there is need for a drug delivery system that enables sequential delivery of multiple growth factors.

Fibroblast growth factor-2 (FGF-2) and bone morphogenetic protein-2 (BMP-2) are two molecules that are best delivered to cells sequentially due to the differing biologic activities of these two factors.[2] The FGF family of growth factors consists of 22 members and FGF-2 has been studied primarily in bone.[9,10] FGF-2 stimulates osteoprogenitor cell proliferation[11] and plays an important role in maintaining bone mass.[12] When FGF-2 is present at high doses or continuously during bone healing, it inhibits bone formation.[2,11,12]

FGF-2 was selected for these studies because of its synergistic effects when used with BMP-2. FGF-2 increases BMP-2 sensitivity of osteoprogenitor cells by upregulating BMP-2 receptor expression and BMP-2 levels.[13,14] Recently, low concentrations of BMP-2 were able to enhance calvarial bone defect repair in transgenic mice overexpressing FGF-2,[15] further confirming that FGF-2 can augment BMP-2-induced bone repair. We reasoned that delivery of FGF-2 initially to stimulate osteoprogenitor proliferation may preclude the use of a high dose of BMP for bone regeneration.[16] BMP-2 is anabolic for bone formation, but clinical studies have shown that high doses of BMP-2 can cause inflammation, ectopic bone formation, osteolysis, seroma formation, and possible increase in the risk of malignancy[17,18]; thus, there is a need to increase efficacy of lower doses of BMP-2.

Our studies in young mice using a codelivery biomaterials system (polyethylene glycol hydrogel on a collagen/hydroxyapatite scaffold) for FGF-2 and BMP-2 failed to show a synergistic effect from the two molecules,[19] leading us to develop a sequential delivery system for FGF-2 and BMP-2. We have recently reported that a poly-L-Lysine/poly-L-Glutamic acid polyelectrolyte multilayer (PEM) film deposited above a biomimetic calcium phosphate (bCaP) layer enables sequential delivery of multiple factors.[20] PEM is a layer-by-layer buildup of oppositely charged polyelectrolytes, a polyanion (−) and polycation (+), to form a thin film that acts as a reservoir to retain bioactivity of electrostatically adsorbed molecules.[21]

PEM films were first introduced 20 years ago for biomedical applications to functionalize surfaces and render them more biomimetic.[22,23] Single bioactive growth factors have been successfully delivered from PEM systems, including osteogenic factors, such as FGF-2, BMP-2, and transforming growth factor beta 1, without the loss of bioactivity.[6,24–30] During the layer-by-layer buildup, the molecules of a PEM film rearrange and thus, incorporated bioactive molecules will also rearrange and get relocated throughout the PEM film.[31] The mixing of the bioactive molecules in PEM-only coatings makes sequential delivery not possible.

The lack of temporal separation of biomolecules in PEM was successfully overcome by the addition of a bCaP barrier layer to the PEM design.[20] A delayed access for 3 days was observed in an *in vitro* cell culture system, but it was unknown if the bCaP-PEM coating could be applied to three-dimensional (3D) scaffolds and function to deliver multiple factors *in vivo*. In this work, we show the benefit of sequential delivery from the bCaP-PEM delivery system on *in vivo* bone formation in adult mice when used to deliver FGF-2 followed by BMP-2 in a critical-sized defect mouse model of bone healing.

Materials and Methods

Cell culture

Mouse mesenchyme-derived progenitor cells were obtained from the femurs of CD1 female mice (3–4 months old) purchased from Jackson Laboratory (Bar Harbor, ME) as described previously.[2] Briefly, aseptically harvested femoral diaphyses that had epiphyses removed and marrow flushed out were chopped into 1 mm^2 fragments, washed, exposed to collagenase II (Invitrogen) for 1.5 h and then washed and seeded into a 100 mm culture dish, and incubated at 37°C in 5% CO_2. Bone chips were initially cultured in Dulbecco's modified Eagle medium (DMEM) (Cat#11995; Gibco) supplemented with 10% FBS (Gibco/Invitrogen, Rockville, MD), 100 U/mL of penicillin-G (Sigma-Aldrich, St. Louis, MO), and 100 mg/mL of streptomycin (Sigma-Aldrich) and replaced twice per week.

After 12–14 days, the cells growing out from the bone fragments reached near confluence and were used for experiments at passage 1. NIH3T3 mouse embryonic fibroblast cells were obtained from American Type Culture Collection (ATTC, CRL-1658, Manassas, VA) and cultured in the same media as the primary cells. At ~80% confluency, both types of cells were trypsinized with 0.25% trypsin and 0.1% EDTA (Gibco) in phosphate-buffered saline (PBS), centrifuged, resuspended, and seeded at 10,000/cm^2 in 100 mm dishes for experiments with FGF-2.

Ratios of heat-inactivated FBS (hiFBS) and non-hiFBS were tested to determine conditions that supported cell proliferation as measured by Alamar Blue, while providing minimal background effects to evaluate effects of FGF-2 addition to the cultures. A total of 10% serum in DMEM medium with antibiotics was used and the effects of 10%, 9%, 8%, 6%, and 5% hiFBS on cell viability were tested. Cell viability was negatively affected with more than 8% hiFBS and the addition of 2% non-hiFBS did not obscure effects on cells from FGF-2 (data available upon request); thus, this ratio of hiFBS:FBS was selected for the studies shown here.

Carrier-free FGF-2 (Cat#233-FB/CF; R&D Systems, Minneapolis, MN) or vehicle was spiked into the medium (5 μL of working stock diluted from 100 μg/mL in 0.1% BSA in saline) on day 1, 3, and 5. FGF-2 doses of 0, 0.0016, 0.016, or 0.16 ng/mL were used. Cells were harvested on day 7 for flow cytometry studies.

Fluorescence-activated cell sorting

Cells were trypsinized and washed in PBS containing 0.2% bovine serum albumin and 0.1% NaN_3. Aliquots containing 10^6 cells were incubated with 100 μL of appropriately diluted antibodies and isotype control antibody for 30 min at 4°C in the dark. The surface antigen panel was selected based on the literature for murine-derived mesenchymal stem cells.[32,33] The following monoclonal antibodies were used for cellular surface staining according to manufacturer's protocols: CD11b (PerCP Cy5.5), CD31 (FITC), and CD45 (Alexa Fluor 700) for hematopoietic cells and CD29 (PE/Cy7), CD44 (Alexa Fluor647), CD166 (PE), and Sca-1 (Pacific Blue) indicators of mesenchyme-derived progenitor stem cells. Antibodies were purchased from eBioscience and Biolegend (San Diego, CA).

Cells were fixed with 2% paraformaldehyde in PBS. Relative fluorescence intensities were determined on a 4-decade

log scale by flow cytometric analysis, using an LSRII (Becton Dickinson, San Jose, CA). At least 1 to 300,000 cell events were collected per sample. Analysis was carried out with FlowJo software (Version7.6.5).

Preparation of biomimetic calcium phosphate/polyelectrolyte multilayer-coated collagen/hydroxyapatite scaffolds

Collagen/hydroxyapatite scaffold. A clinically used bone graft substitute, Healos® (DePuy Synthes Spine, Raynham, MA), was used as the base scaffold for these studies and was obtained from the manufacturer as a sheet that was then cut to size for the mouse experiments. Healos is a porous, fibrous scaffold made of 70% collagen and 30% hydroxyapatite and is nearly radiolucent allowing for discrimination of new bone formation by microcomputed tomography (micro-CT). Using a 3.5 mm biopsy punch (Integra Miltex, York, PA), scaffolds were cut out of a sheet of Healos that had been trimmed to 1 mm thickness and then UV sterilized for 10 min on each side before BMP-2 adsorption and deposition of the calcium phosphate and PEM layers. This scaffold size was selected since it is the same size as the mouse calvarial bone defect.

Application of BMP-2 and bCaP. BMP-2 (2 μg) (Biologics Corp., Indianapolis, IN) was applied to the porous Healos scaffolds by pipetting 2 μL of 1 mg/mL stock made in PBS on each scaffold and allowing it to adsorb for 1 h at room temperature without drying completely. A two-step SBF method[34] was then used to deposit a carbonated apatite layer over the BMP-2. As described previously, an amorphous CaP layer was first allowed to nucleate on the scaffold by immersion in SBFx5 Solution A, which was then covered by a uniform nanocrystalline bone-like carbonated apatite layer by immersion in SBFx5 Solution B, and visualized by scanning electron microscopy (SEM).[34]

The 3.5 mm diameter × 1 mm thick Healos scaffolds (up to 10) were added to 300 mL of SBFx5 Solution A in a beaker equipped with a stir bar. The beaker was covered with plastic film with 20–30 holes punched into it and placed on a stir plate (~130 rpms) in a 37°C oven. After ~24 h, the beaker was removed from the oven and sonicated (with scaffolds still in reacted Solution A) for 10 s to remove loosely bound crystals. Scaffolds were transferred to another beaker containing 300 mL of Solution B SBFx5.[34] After 16 h with stirring in a 50°C oven, scaffolds were sonicated in reacted Solution B for 10 s and then rinsed thrice with saline before initiating PEM coating.

BMP-2 enzyme-linked immunosorbent assay (ELISA) analysis of reacted Solution A and Solution B was used to determine the BMP-2 dose on the scaffold. It was found that ~65% of total BMP-2 loading on scaffold was washed off in the 300 mL volume of SBFx5 Solution A. The BMP-2 dose remaining on the bCaP-PEM scaffolds after bCaP deposition was thus 0.7 μg.

Scanning electron microscopy. The uniformity and morphology of the bCaP deposited on and within the porous scaffolds after Solution A and Solution B precipitation were characterized using SEM (JSM—5900LV; Jeol USA, Inc., Peabody, MA). After the coating process, the scaffolds ($N = 3$) were cut in half, allowing the examination of the coating within the pores in cross-section. Previous characterizations of the mineral formed by this deposition process had confirmed the reliable precipitation of a single phase of carbonated apatite with a distinctive morphology[20,34]; thus X-ray spectroscopy and chemical composition were not repeated for this study, and SEM and micro-CT were only used to confirm the bCaP coating throughout the scaffold.

Application of PEM and FGF-2. To form the layer-by-layer PEM coating, the bCaP-coated scaffolds were alternately immersed for 10 min in 300 μL of 1 mg/mL poly-L-Glutamic acid or poly-L-Lysine solution in saline with three saline rinses between. Loosely bound or unbound polyelectrolytes must be completely rinsed out before changing to the alternate polyelectrolyte solution to maintain the layer-by-layer buildup and avoid particulate precipitation. Simple immersion in saline was not adequate for the electrolyte solution to be rinsed out of the pores deep within the scaffold; thus a centrifuge step was employed to remove the PEM solutions from the pores between each solution change.

The scaffold was placed in a 1.5 mL centrifuge tube with a 0.65 μm filter-membrane insert (Cat# UFC40DV25; EMD Millipore, Billerica, MA). These microcentrifuge tubes are made up of two compartments separated by a membrane. This allows the sample to rest on the filter insert submerged in electrolyte or rinse solutions until tubes are centrifuged for ~10 s at 1000 rpm. Centrifugation forces the excess solution out of the pores of the scaffold and through the membrane, leaving the scaffold ready for the next solution immersion. This procedure was repeated until 30 bilayers of PEM were adsorbed (1 bilayer = PLGlut+PLLys). The bCaP barrier and number of PEM bilayers were selected based on previous *in vitro* data showing that PEM with a bCaP barrier layer enabled sequential delivery of multiple factors.[20]

After PEM application, a 100 μg/mL frozen stock of FGF-2 was diluted with saline without BSA to a 5 μg/mL working stock and 2 μL (10 ng) was applied to each scaffold that had been spun nearly dry by centrifugation in the filter tubes and allowed to bind for 1 h, while sealed at room temperature. The scaffold was then put in 300 μL DMEM (Cat# 11995; Gibco/Invitrogen) for 1 h and then centrifuged in the filter tubes just before implantation to remove the DMEM. The absence of BSA in the FGF-2 solution was critical to increase the binding affinity of FGF-2 to the charged polyelectrolyte components in PEM. Enzyme-linked immunosorbent assay (human FGF-2 ELISA; R&D Systems, Minneapolis, MN) measurements of the DMEM rinse solution were used to determine FGF-2 dose remaining on the scaffold and was found to be 50% or 5 ng. The thickness of the bCaP-PEM layer is ~16.3 + 2.2 μm based on our previous publication.[20]

In vivo *osteogenesis assays with a mouse calvarial defect model*

All animal experimental procedures were approved by the Animal Care and Use Committee of UConn Health Center, Farmington, CT, before initiating animal studies. Transgenic Type I collagen female reporter mice at 4–7 months of age (with a CD1 background and Col 3.6-cyan fluorescence)[35] were bred in-house and used for the bone regeneration studies due to their enhanced capability for identifying bone formation. Mice in this age range were used because they are considered skeletally mature.[36]

Mice were anesthetized with 90 mg/kg ketamine and 9 mg/kg xylazine through intraperitoneal injection. In each mouse, a single, critical-sized 3.5 mm diameter hole[37] was created in the center of one of the two parietal bones using a trephine and avoiding cranial sutures, which can inhibit bone formation. A coated scaffold with or without growth factors was placed in the defect. The periosteum and subcutaneous tissue were closed with sutures, followed by suturing the skin incision.

Mice were given 0.08 mg/kg buprenorphine through intramuscular injection for pain management for 3 days postsurgery. Mice were euthanized by asphyxiation with carbon dioxide after 1 or 3 weeks postsurgery and calvarial bones were harvested. The 1-week time point was selected to evaluate early proliferative effects from FGF-2; therefore all mice in these groups ($N = 3$ mice/group) received peritoneal cavity injections of 3 μg/g EdU (5-ethynyl-2-deoxyuridine, a nucleoside analog of thymidine, Click-iT EdU imaging kit, C10339; Invitrogen) 1 day before euthanasia.

Tissue sections were immunostained to detect Sca-1 and CD166 positive cells, which are progenitor cell markers and shown to be the primary cell population responding to FGF-2 in our *in vitro* studies. All mice in the 3 week time point groups received peritoneal cavity injections of 3 μg/g calcein and alizarin complexone calcium labels before sacrifice at 7 days and 1 day, respectively. For the calvarial defect studies, four mice/group were used for test groups and five mice were used for the negative control.

Tissue immunofluorescence staining

Calvarial bones were harvested and fixed in 10% neutral buffered formalin solution at 4°C for 2–3 days and prepared for cryohistological analysis, as described previously, to determine if the newly formed bone was positive for Type I collagen expression and a variety of immunostains associated with bone formation.[38] Cross-sections were cut perpendicular to the plane of the bone surface and were obtained from the center of the defect to best examine the central area of the defect that is the most difficult to heal. After a section was imaged for endogenous fluorescent signals (scaffold and bone mineral calcium staining, and Collagen Type I-cyan GFP-positive cells), the cover slide was removed by brief soaking in PBS and then processed for additional staining.

For alkaline phosphatase (AP) and tartrate-resistant acid phosphatase (TRAP) staining, the sections were first stained for the TRAP activity using ELF97 (E6589; Life Tech) as the fluorescent substrate (yellow). The same slides were placed again in PBS and then stained for the AP activity using fast red substrate (#F8764-5G; Sigma-Aldrich,) and DAPI (#D-1306; Mol Probes), and reimaged.

The TRAP signal was segmented with a filter optimized for tetracycline (HQ409sp, 425dcxr, HQ555/30, set lot C-104285; Chroma Technology Custom). The alizarin complexone mineralization line was captured utilizing a TRITC filter (49005ET; Chroma Technology), and FITC was captured with a YFP filter (49003; Chroma Technology). The fluorescent images were captured by an AxioCam MRm Rev.3 monochromatic camera, whereas the chromogenic sections were recorded with a Hitachi HV-F202 brightfield camera.

For immunohistochemistry of progenitor cell markers Sca-1 and CD-166, sections were incubated with primary antibody against CD166 (1:250, Cat#14-1661-81; eBiosicience) and Sca-1 (1:250, catalog Cat#122501; Biolegend) overnight at 4°C. Section were washed with PBS and a secondary antibody anti-rat IgG TRITC (1:500, Cat#26-4826-82; eBiosicience) was added, and slides were incubated at room temperature for 1 h in a dark humidified chamber. Sections were counterstained with DAPI and coverslipped with PBS and glycerol. Images of a single section taken in the middle of the defect were analyzed by ImageJ to determine percentage of positive immunostained area relative to DAPI.

X-ray and micro-CT imaging

Mineralized bone volume within the retrieved calvarial defect sites was quantified using conebeam microfocus X-ray computed tomography (μCT40; ScancoMedical AG, Bassersdorf, Switzerland) as described previously.[19] Serial tomographic images were acquired at 55 kV and 145 μA, collecting 1000 projections per rotation at 300 ms integration time on fixed tissue samples before decalcification for histology. Three-dimensional 16-bit grayscale images were reconstructed using standard convolution back-projection algorithms with Shepp and Logan filtering, and rendered within a 16.4 mm field of view at a discrete density of 244,141 voxels/mm^3 (isometric 16-μm voxels). Segmentation of bone from scaffold and marrow and soft tissue was performed in conjunction with a constrained Gaussian filter to reduce noise.

New bone was analyzed by selecting volumetric regions manually by visual inspection of each two-dimensional (2D) cross-section to include all new bone formation, whether it formed within the circular defect space or grew from the adjacent original calvarial bone surface. Calvarial bone samples were X-rayed using a Faxitron MX-20 X-ray cabinet (Faxitron). Images were acquired using a 28 kV setting for 4-s exposure at a distance of 20.9 cm from the source. The images were then captured and stored using the Faxitron DX software (version 1.00).

Statistics

For *in vitro* studies, analysis of variance (ANOVA) followed by Newman–Keuls multiple comparison tests were performed. At least three independent experiments from different isolations of cells from bones, from at least three mice were performed. The statistical analysis of the two groups in the 1-week *in vivo* results was performed by unpaired two-tailed Student *t*-test with $p < 0.05$ considered statistically significant. The three *in vivo* 4-week samples were analyzed by ANOVA followed by Tukey's multiple comparisons test with significance set at $p < 0.05$. Data are expressed as mean ± SD.

Results

As way to understand a possible mechanism of action of FGF-2 on bone progenitor cells, *in vitro* studies with murine bone chip outgrowth cells and NIH3T3 murine fibroblast control cells were conducted in which FGF-2 was spiked into the media. Fluorescence-activated cell sorting (FACS) analysis for a panel of typical mesenchymal stem cell markers was performed on day 0 (D0) and day 7 after 6 days of FGF-2

Table 1. Surface Marker Analysis of Mesenchyme-Derived Progenitor Cells from Mouse Bone Fragments and NIH3T3 Fibroblasts (3T3) Before and After FGF-2 Treatment

Day and ng/mL FGF-2	*Cell type*	*CD11b%*	*CD31%*	*CD45%*	*CD29%*	*CD44%*
D0 0.0	MDPC	54.3 ± 2.1	0.0	64.3 ± 2.1	94.0 ± 3.0	84.0 ± 16.2
	3T3	0.0	0.0	0.0	99.6 ± 0.2	27.7 ± 5.3
D7 0.0	MDPC	31.7 ± 14.6	0.0	28.5 ± 16.9	87.7 ± 0.7	50.0 ± 26.3
	3T3	0.0	0.0	0.0	>99.5	8.1 ± 6.2
D7 0.0016	MDPC	32.2 ± 16.5	0.0	29.7 ± 17.7	91.7 ± 2.6	50.0 ± 26.3
	3T3	0.0	0.0	0.0	>99.5	8.3 ± 7.0
D7 0.016	MDPC	29.8 ± 12.5	0.0	28.6 ± 13.2	92.1 ± 4.6	69.4 ± 23.7
	3T3	0.0	0.0	0.0	>99.5	5.9 ± 6.8
D7 0.16	MDPC	27.0 ± 10.2	0.0	23.9 ± 14.2	91.5 ± 4.2	72.2 ± 20.4
	3T3	0.0	0.0	0.0	>99.5	15.2 ± 9.3

FGF-2, fibroblast growth factor-2; MDPC, mesenchyme-derived progenitor cell.

exposure (Table 1). Neither cell type expressed the hematopoietic marker CD31 at the two time points tested. The macrophage marker, CD11b, was expressed at 54% on D0 in the progenitor cells from mouse bone chips, but decreased to 32% by D7, while NIH3T3 fibroblasts did not express CD11b. CD45, another hematopoietic cell marker, was also positive in the bone chip cells, but negative in the NIH3T3 fibroblasts. The cells from mouse bone chips are primary cells and hematopoietic cell contamination is unavoidable, yet can be reduced with repeated cell culture passaging that was not conducted in these studies.[32]

Regarding the murine MSC markers, CD29 was highly expressed in both cell cultures. CD44 was 84% on D0 in the cells from mouse bone and remained at 50% or higher over time. However, the NIH3T3 fibroblasts had 28% CD44 on D0 and this percentage decreased to 8% by D7. On D0, the NIH3T3 fibroblasts also expressed a small percentage of Sca-1 and CD166, 25.2% and 3.1%, respectively, which was less than in the cell cultures derived from mouse bone, 30.0% and 12.4%, respectively (Fig. 1A, B).

When both cell types were stimulated with different concentrations of FGF-2, none of the hematopoietic or MSC markers shown in Table 1 were affected significantly by FGF-2 in cells from mouse bone or the NIH3T3 fibroblasts. Varying doses of FGF-2 (0.0016, 0.016, or 0.16 ng/mL) had no significant effect on CD166 and Sca-1 in NIH3T3 fibroblasts. However, the primary cells from mouse bone demonstrated a significant dose-dependent increase in CD166 and Sca-1 positive cells due to FGF-2 supplementation (Fig. 1A and B, respectively).

In order for the bCaP barrier layer coating to be applied uniformly within the pores of the commercially available bone graft, it was necessary to stir each of the two simulated body fluid solutions and allow the scaffolds to move freely through the solution during bCaP deposition. The micro-CT images and SEM images (Fig. 2) show successful deposition of the coating throughout the scaffold. The scaffold density increased uniformly after incubation in the SBFx5 solutions relative to the as-received scaffold (Micro-CT images in Fig. 2i vs. v). The SEM micrographs (Fig. 2B) show that the porous fibrous structure of the scaffold is retained after bCaP deposition and at the highest magnification, the presence of the bCaP nanocrystalline coating is visible relative to the control as-received sample (Fig. 2B-viii vs. iv).

To ensure PEM solutions uniformly coated the internal pores of the bCaP-coated scaffolds, it was necessary to spin out each solution at every step of the process by placing the sample on a filter insert in a microcentrifuge tube.

Given the previously observed proliferative effects of FGF-2 *in vitro*,[39] the proliferative effects of FGF-2 *in vivo* when delivered from the bCaP-PEM coated scaffold with

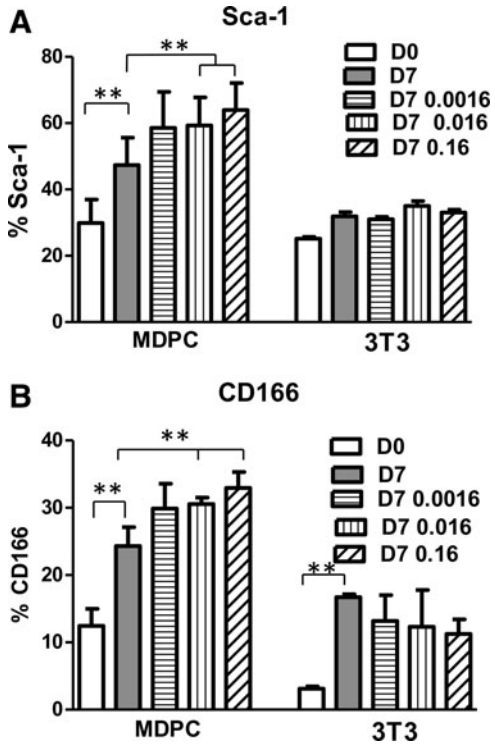

FIG. 1. Addition of FGF-2 to cultures of MDPCs from mouse bone fragments and NIH3T3 mouse fibroblasts (3T3) had different effects on Sca-1 and CD166 markers, as measured by flow cytometry analysis. **(A)** MDPC cultures had an FGF-2 dose-dependent increase in the expression of Sca-1 on D7, compared to D0 baseline and vehicle-treated D7 cultures. 3T3 cells did not respond to FGF-2 in a significant manner. FGF-2 doses shown on graph legend are expressed in ng/mL. $^{**}p \leq 0.01$. **(B)** MDPC exhibited an FGF-2 dose-dependent increase in the expression of CD166 on D7, compared to D0 and vehicle-treated D7 cultures. 3T3 cells did not respond to FGF-2 in a significant manner. FGF-2 doses expressed in ng/mL. $^{**}p \leq 0.01$. FGF-2, fibroblast growth factor-2; MDPC, mesenchyme-derived progenitor cell.

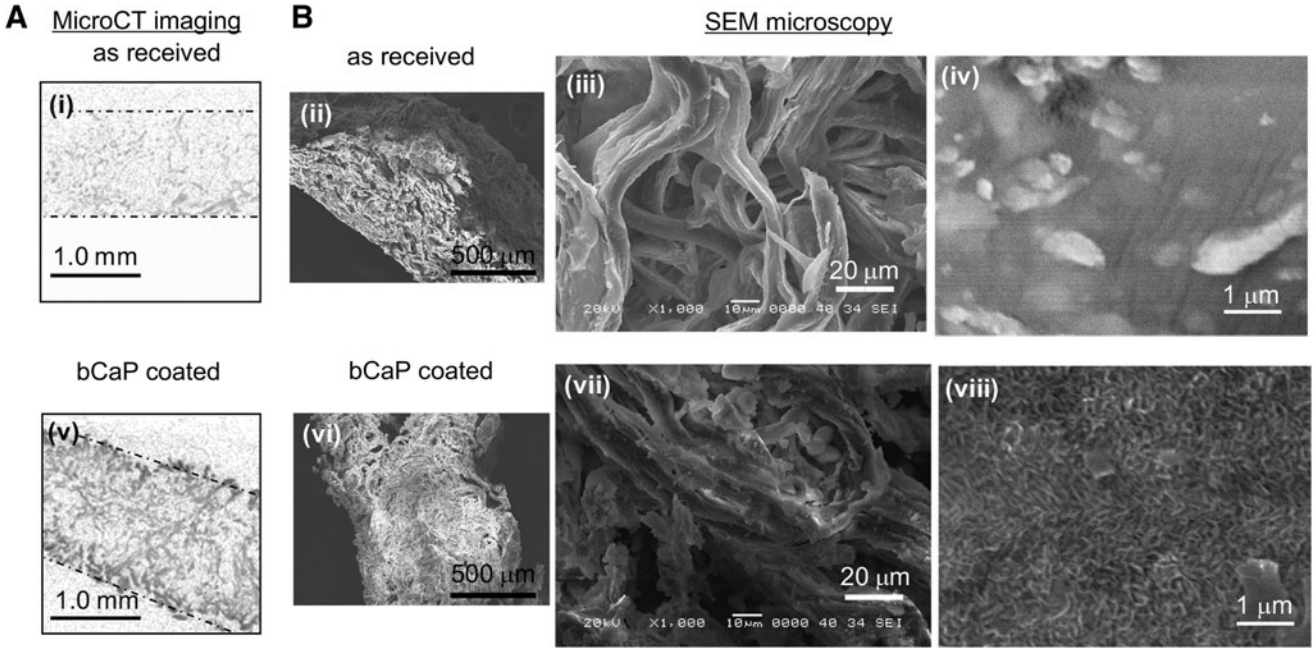

FIG. 2. Micro-CT imaging and SEM confirm uniform coating of the collagen/hydroxyapatite scaffold by the bCaP deposition method. **(A)** The as-received scaffold is nearly radiolucent and barely visible by Micro-CT (*dotted lines* outline the scaffold), (i) while after bCaP coating, the scaffold became denser and radio-opaque throughout (v). **(B)** SEM images of cross-sections of the scaffold at a variety of magnifications show that the porous structure is retained during bCaP deposition (ii–viii). Fibers are present in as-received material (iii) and after bCaP coating (vii). The distinctive nanocrystalline structure of the carbonated apatite layer formed by the bCaP simulated body fluid method can be seen in (viii) after the bCaP coating process relative to uncoated scaffold (iv). bCaP, biomimetic calcium phosphate; micro-CT, microcomputed tomography; SEM, scanning electron microscopy.

BMP-2 were evaluated at 1 week after implantation in the mouse calvarial defect. Figure 3A shows a schematic of the tissue cross-section taken through the calvarial bone defect and scaffold that was studied. The box drawn around the central defect area is the most difficult to heal and thus of most interest. Figure 3B are images of the frozen histological sections labeled with DAPI and EDU, with a box indicating the area of higher magnification shown in Figure 3C. An increase in proliferating EdU-labeled cells was observed at 1 week in the center area of scaffolds with FGF-2 and BMP-2 relative to BMP-2 alone indicating successful delivery of active FGF-2 from the bCaP-PEM coating (Fig. 3D).

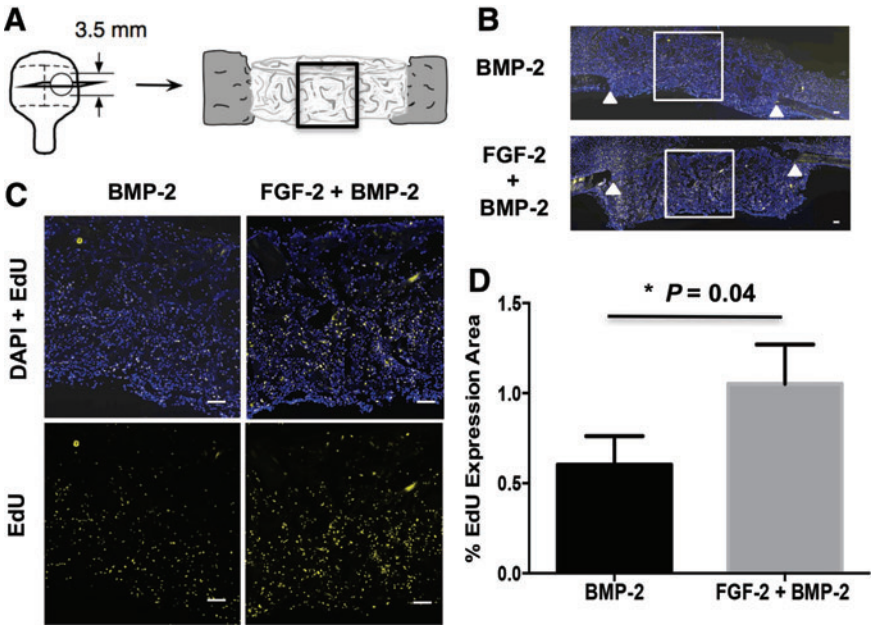

FIG. 3. One-week evaluation of cell proliferation resulting from *in vivo* FGF-2 delivery by the bCaP-PEM coated scaffold. **(A)** Schematic representation of the 3.5 mm critical-sized calvarial bone defect showing the histological sectioning and central defect region analyzed. **(B)** Fluorescence images of the entire calvarial defect showing DAPI stained (*blue*) and EdU-labeled (*yellow*) cells with *white triangles* indicating original bone defect edges. *White box* indicates area of higher magnification shown in **(C)**. **(C)** Higher magnification images show increased EDU staining in scaffolds with FGF-2 and BMP-2 compared to BMP-2 alone. **(D)** Quantified results from Image J analysis of the histological sections shown in **(C)**. Scale bar = 200 μm. BMP-2, bone morphogenetic protein-2; PEM, polyelectrolyte multilayer. Color images available online at www.liebertpub.com/tea

To understand if the cells proliferating in response to FGF-2 delivery were the desired progenitor cells, immunohistochemistry was conducted. There was a demonstrated increase in Sca-1+ progenitor cells with FGF-2+BMP-2 compared to BMP-2 alone (Fig. 4). While CD166+ progenitor cells increased *in vitro* in response to FGF-2, positive CD166 staining was not observed *in vivo* at this dose of FGF-2 when delivered from the bCaP-PEM coated scaffolds.

The effects of FGF-2 and BMP-2 delivered from the bCaP-PEM scaffold were evaluated at 3 weeks in the mouse calvarial bone defect model. Examination of the freshly excised tissue and radiographs combined with micro-CT images qualitatively demonstrated increased bone formation due to implantation of the sequential delivery system containing both FGF-2 and BMP-2 relative to BMP-2 only or scaffold alone (Fig. 5A). In addition, the 2D micro-CT cross-sections show that more bone was formed in the center of the defect when FGF-2 was present (Fig. 5A-iv). More bone formation in the center of the scaffold also correlated with the increased number of Sca-1+ cells in the center of the scaffold (Fig. 4). Quantification of bone volume by micro-CT shows a significant increase in total bone volume with sequential delivery of FGF-2+BMP-2 in bone defects compared to BMP-2 alone (Fig. 5B).

To distinguish true bone formation from the bone-like calcium phosphate-coated scaffold, histological analysis was conducted with a focus on verifying active osteoblast deposition of bone using a combination of techniques. Active bone mineralization was demonstrated by positive labeling with calcein (green) and alizarin complexone (red) shown in Figure 6A, low magnification, and Figure 6B, high magnification. Collagen reporter positive cells shown in blue were found adjacent to the mineralization lines particularly in the BMP-2 and FGF-2+BMP-2 treated groups, which had increased bone formation relative to the scaffold-only control (Fig. 6B yellow arrows). The control scaffold with vehicle alone did not stimulate bone healing as evidenced by a lack of Type I collagen reporter cells and minimal calcium deposition (Fig. 6B first column).

The greatest new bone formation occurred in the FGF-2+BMP-2 samples compared to controls of BMP-2 only and scaffold without growth factors. The presence of new bone in the implanted scaffold was further confirmed in the nonfluorescent toluidine blue-stained sections (Fig. 6C). The areas of active mineralization exhibited increased AP staining, which indicates the presence of osteoblasts and active bone formation (Fig. 6D). TRAP staining was most intense in the areas adjacent to the original bone defect, demonstrating active osteoclasts involved in bone and scaffold resorption and bone remodeling (Fig. 6E).

Discussion

These studies with a novel bCaP-PEM coating capable of sequential delivery applied to a commercially available bone graft substitute demonstrate that FGF-2 delivery followed by BMP-2 increases bone regeneration in adult mouse calvarial bone defects more than delivery of BMP-2 alone. Both the *in vitro* studies with mouse bone chip outgrowth cells and the *in vivo* studies with this new coating technology suggest that the main mechanism for this anabolic effect is the early FGF-2-induced proliferation of a pool of osteoprogenitors, particularly Sca-1 positive cells.

FACS was used to characterize the *in vitro* cell cultures of mouse bone chip outgrowth cells and their changes in response to FGF-2. FGF-2 uniquely expanded the Sca-1 and CD-166 positive populations in the *in vitro* cultures of the bone chip outgrowth cells. *In vivo*, Sca-1+ labeled osteoprogenitors were found to be more prevalent in the center of the scaffold early in bone regeneration at 1 week when FGF-2 was delivered with BMP-2 compared to scaffolds with BMP-2 alone. This was followed by the observation of increased bone formation in the center of the scaffold at 3 weeks, verifying the importance of the Sca-1+ progenitors in bone healing and the role of FGF-2 in stimulating bone formation by proliferation of these cells.

The positive results obtained in this study were due to the capacity of the bCaP coating to sequentially deliver the factors and prevent concurrent release of FGF-2 and BMP-2. Our previous *in vivo* calvarial defect studies[19] demonstrated that concurrent codelivery of 2 μg BMP-2 and 5 ng FGF-2

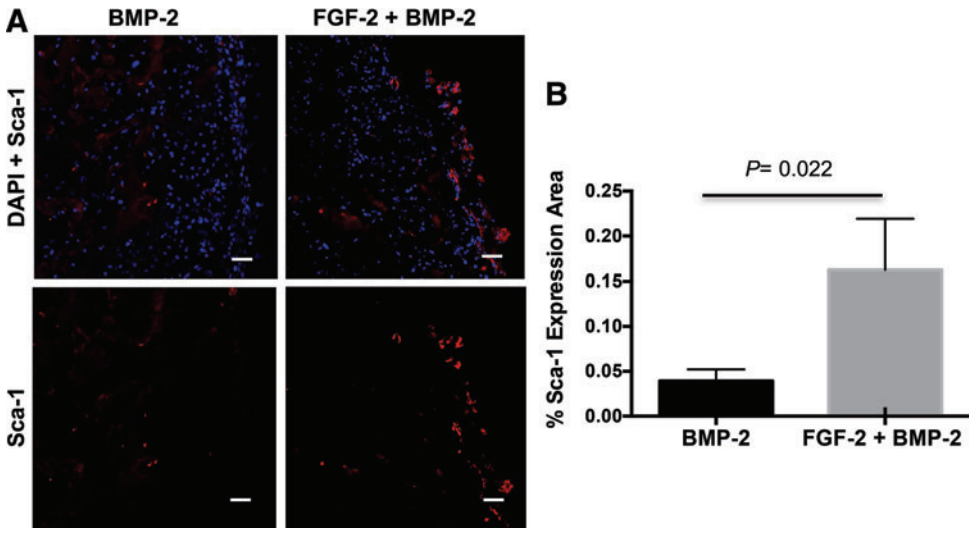

FIG. 4. One-week immunostaining evaluation of progenitor cell recruitment from *in vivo* FGF-2 delivery by the bCaP-PEM coated scaffold. **(A)** Fluorescence images of DAPI (*blue*) and Sca-1 (*red*) stained cells in mouse calvarial bone defects show increased Sca-1 staining with the addition of FGF-2 to BMP-2 compared to BMP-2 alone. **(B)** Graph showing quantified results from Image J analysis with significant increase of Sca-1+ progenitor cells compared to BMP-2 alone in the center of the scaffold. Color images available online at www.liebertpub.com/tea

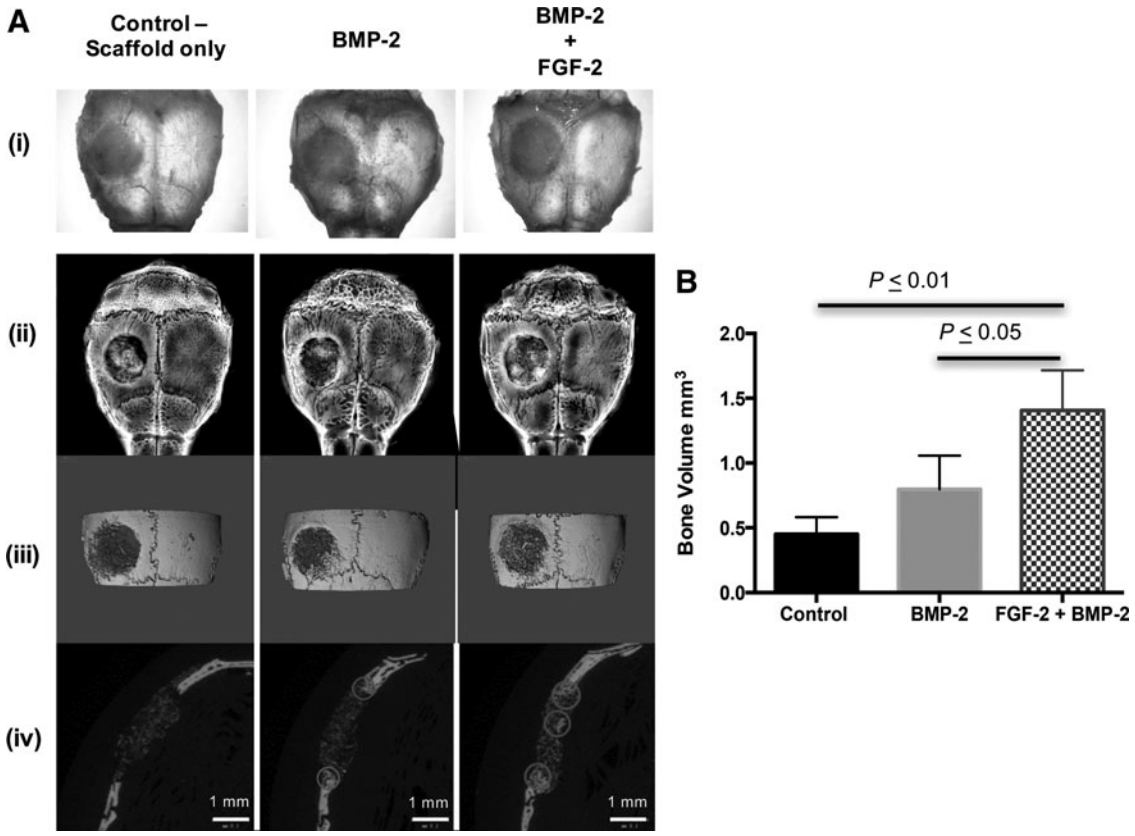

FIG. 5. *In vivo* mouse calvarial bone defect repair at 3 weeks after implantation of bCaP-PEM coated collagen/hydroxyapatite scaffolds treated with vehicle, BMP-2, and BMP-2 and FGF-2. **(A)** (i) Photographs of freshly excised calvarial bones, (ii) radiographs, (iii) representative three-dimensional micro-CT reconstructions, and (iv) corresponding two-dimensional micro-CT scans from which bone volume was determined. Examples of new bone formation are circled. **(B)** Significant increases in new bone volume in the defect area were observed with BMP-2 and FGF-2 compared to BMP-2 only and control. Mean ± standard deviation is plotted.

should be avoided because it did not increase bone formation in mice of a similar age to those used in this study. Our previous *in vitro* studies also showed inhibition of osteogenesis from concurrent codelivery of FGF-2 and BMP-2 in bone chip outgrowths from young mice.[2]

Other groups have also shown that codelivery of FGF-2 and BMP-2 from colloidal gelatin gels can have inhibitory effects on *in vivo* bone formation when compared to BMP-2 alone.[40] Nakamura *et al.* hypothesized that high-dose FGF-2 stimulated inhibitors of BMP-2 signaling (Smad 6) or stimulated osteoclastogenesis that led to decreased bone formation or bone density.[41] Inhibition of bone regeneration was also seen when FGF-2 and BMP-2 were administered as bolus injections without a biomaterial in a rat mandible defect: codelivery of factors was significantly worse at inducing bone apposition compared to BMP-2 alone, and was comparable to the control that was not treated with any growth factors.[42] In contrast, the sequential delivery of FGF-2 first followed by BMP-2 when spiked into cell cultures has been shown to result in an enhanced *in vitro* osteogenesis over codelivery or single factor delivery, providing a sufficiently low dose of FGF-2 in the nanogram range used.[2,43–45]

The main challenge in achieving positive results *in vivo* from FGF-2 and BMP-2 has been the lack of a delivery system capable of sequential delivery of factors without an initial partial low-dose delivery of the second factor at time zero. Many reports about multifactor drug delivery systems claim sequential delivery profiles, when upon closer examination, it can be seen that both factors are released simultaneously, but at different rates.[4,40, 46–49] Notably, Lei *et al.*[50] developed sequential delivery core-shell microspheres, in which FGF-2 and BMP-2 were encapsulated in either the core or the shell. Their *in vitro* studies demonstrated that the truly sequential delivery of first FGF-2 from the shell and then BMP-2 from the core induced osteogenic differentiation of human MSCs better than the growth factors delivered in parallel. This study has now shown *in vivo* efficacy of a cell-free sequential delivery, bCaP-PEM system, which stimulated endogenous cells.

The bCaP-PEM coating delivery system is very different from polymeric systems such as the core-shell microspheres that freely release the factors in easily measurable quantities. The ELISA release studies could not detect release of BMP-2 from bCaP-PEM coatings into media, most likely due to the fact that the bCaP coating process leads to wash-off of 70% of the initially adsorbed BMP-2 and the PEM process further washes off any weakly bound BMP-2. Factors adsorbed below the bCaP-PEM require direct cell

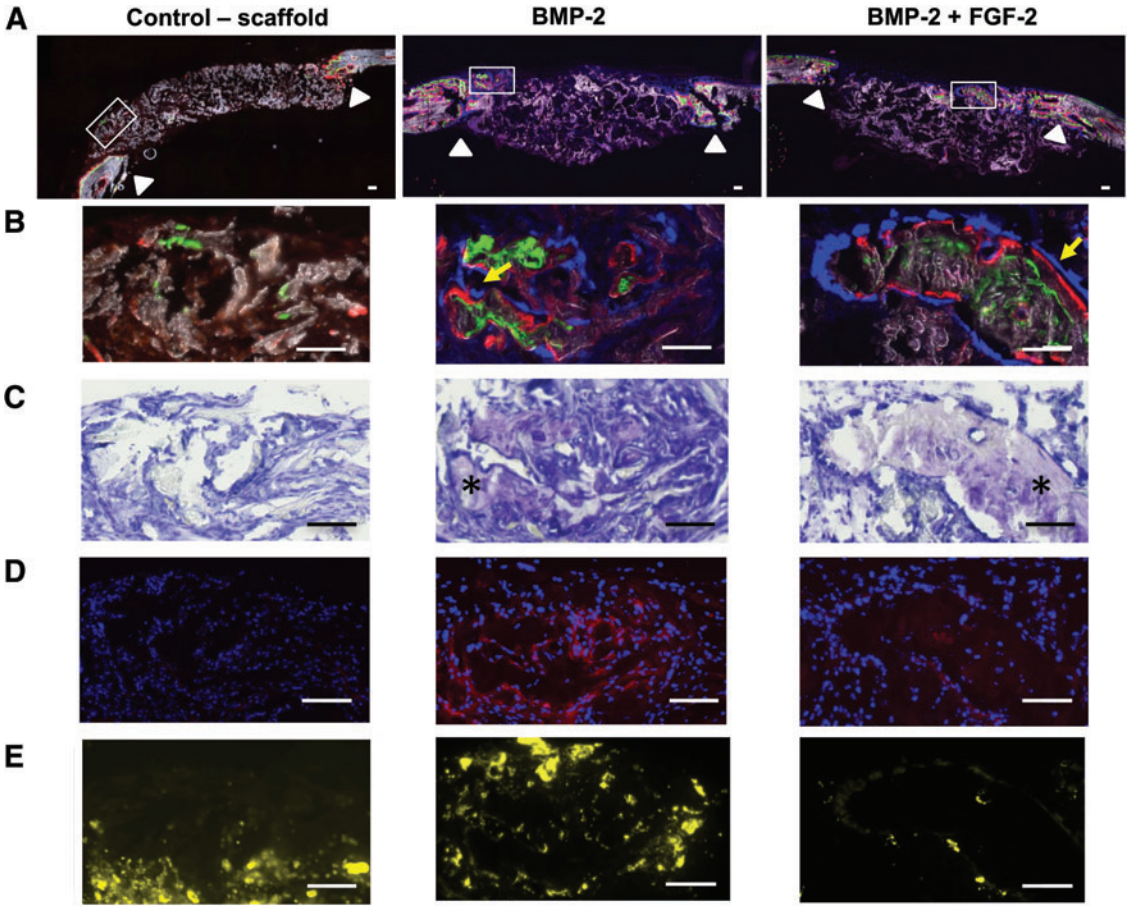

FIG. 6. Histology images of the mouse calvarial bone defect after 3 weeks of scaffold implantation demonstrate new bone formation distinct from the original collagen/hydroxyapatite scaffold and enhanced bone formation in the central defect area with the addition of FGF-2 to BMP-2. **(A)** Low magnification images of the entire defect have a *white box* that indicates the region shown at high magnification in the rows below. The *white triangles* indicate the original bone defect edges. Only the FGF-2+BMP-2 group had new bone present in the center of the defect. Scale bar = 200 μm. **(B)** Active bone mineralization during the last week of implantation is shown by calcein green and alizarin red complex one staining in the groups with BMP-2, but not the control scaffold. *Blue* cells present in the BMP-2 and FGF-2+BMP-2 group are matrix-producing osteoblasts as indicated by positive cyan Type I collagen reporter expression and their location adjacent to freshly stained mineral (*yellow arrows*). **(C)** Toluidine blue staining confirms typical histological features of bone (marked with an asterisk) in the areas with active mineral and ALP staining in the BMP-2 and FGF-2+BMP-2 groups. **(D)** Alkaline phosphatase staining, ALP (*red*), is a feature of matrix-producing osteoblasts and found in the BMP-2 and FGF-2 and BMP-2 groups. Cell nuclei stained *blue* with DAPI. **(E)** Tartrate-resistant acid phosphatase (TRAP) staining, (*yellow*) reveals substantial osteoclast activity near the original defect edges in the scaffold-only group and the BMP-2 only group. The bone formation in the central area of the FGF-2 treated groups does not yet have TRAP staining at the same level of the BMP-2 group, indicating it is newer and less mature. Scale bar = 200 μm for all high magnification images. TRAP, tartrate-resistant acid phosphatase. Color images available online at www.liebertpub.com/tea

interaction with the coating to get access to the factors. The bCaP-PEM is thus a highly localized delivery system that is ideal for delivery of factors with unwanted side effects when delivered systemically such as BMP-2.

One challenge with the use of bCaP on a collagen/hydroxyapatite (Healos) scaffold as a component of a delivery system for osteoinductive factors is distinguishing the new bone formation from the scaffold due to the similarity of bone mineral with the scaffold components. In this case, the Type I collagen reporter mice[35] are an ideal model system to use since verification of osteoblastic cellular activity can easily be accomplished. Furthermore, the use of an ALP immunostain and TRAP staining provided additional verification of the appropriate osteoblastic cellular activity in addition to mineral deposition and Type I collagen reporter expression. This rigorous combination of methods ensures that new bone formation can be conclusively demonstrated as a distinct entity from the bCaP scaffold material.

The *in vitro* studies compared responses of two different cell types to FGF-2 to identify which markers to look for in the *in vivo* studies. Surprisingly, the studies resulted in the discovery that the bone progenitor cells derived from bone chip outgrowths could be distinguished from fibroblasts by their expression of CD44, Sca-1, and CD166, but not by CD29, which was expressed by both cell types. Sca-1 has been identified as a marker for stem cells and progenitor

cells,[51] while CD166 or activated leukocyte cell adhesion marker is a stem cell marker that has been relatively ignored in the bone field since its initial identification in 1998.[52] In these studies, only the bone chip outgrowth cells responded to FGF-2 stimulation by increasing Sca-1+ and CD166+ populations, not the fibroblasts. Given the confusion in the field regarding how to distinguish a progenitor cell that can make bone from a nonbone forming fibroblast,[53] testing responsiveness to FGF-2 through Sca-1 and CD166 may be a useful strategy for others attempting to isolate a population of bone progenitor cells.

Conclusion

The sequential delivery of multiple biological factors in the order that mimics the natural biological process is an emerging strategy to enhance osteogenesis and tissue regeneration. The bCaP-PEM coating process is a system that enables highly localized, sequential delivery of factors. The PEM layer serves as a reservoir for a biomolecule like FGF-2 intended to provide an initial tissue regeneration cue such as cell migration or proliferation. The bCaP barrier layer blocks the premature release of a different bioactive factor; such as BMP-2, adsorbed to the scaffold intended to provide a secondary cue to cells during the regenerative process.

This study shows that bCaP-PEM can be applied throughout 3D porous scaffolds, clinically used for bone grafting. The sequential FGF-2/BMP-2 delivery profile from the bCaP-PEM coating was able to increase bone formation in adult mice. This is an improvement over our previous work in which a polyethylene glycol hydrogel layer that co-delivered FGF-2 and BMP-2 inhibited bone formation in adult mice.[19]

The mechanism behind the enhanced bone formation from FGF-2 and BMP-2 was investigated through *in vitro* testing with bone chip outgrowth cells combined with flow cytometric analysis and 1-week *in vivo* calvarial bone implant retrievals. These studies revealed an osteoprogenitor cell population responding to FGF-2 that was mirrored in the *in vivo* studies and supported the hypothesis that expansion of an osteoprogenitor pool of cells before delivery of an osteoinductive agent is an important strategy to maximize bone formation. To summarize, biomimetic delivery of multiple growth factors through a biomaterial coating creates a cell-instructive scaffold that is a strategic approach for maximizing osteoinduction that avoids complications of cell-based therapy. This versatile coating technique can be used to test the impact of sequential delivery of a variety of combinations of factors to enhance bone tissue regeneration.

Acknowledgments

Funding was provided from the National Institutes of Health, National Institute of Dental and Craniofacial Research (NIDCR) R01DE021103. The content is solely the responsibility of the authors and does not necessarily represent the official views of the National Institutes of Health. The authors would like to thank Dr. Liping Wang for conducting the animal surgeries and Li Chen for conducting the bone histology in the Imaging Core Service Center at UConn Health under the direction of Dr. David Rowe. We would also like to acknowledge the use of the Micro-CT Imaging Facility at UConn Health under the direction of Dr. Douglas Adams.

Disclosure Statement

No competing financial interests exist.

References

1. Jiang, B., Zhang, G., and Brey, E.M. Dual delivery of chlorhexidine and platelet-derived growth factor-BB for enhanced wound healing and infection control. Acta Biomater **9,** 4976, 2013.
2. Kuhn, L.T., Ou, G., Charles, L., Hurley, M.M., Rodner, C.M., and Gronowicz, G. Fibroblast growth factor-2 and bone morphogenetic protein-2 have a synergistic stimulatory effect on bone formation in cell cultures from elderly mouse and human bone. J Gerontol A Biol Sci Med Sci **68,** 1170, 2013.
3. Lee, A.L., Wang, Y., Cheng, H.Y., Pervaiz, S., and Yang, Y.Y. The co-delivery of paclitaxel and Herceptin using cationic micellar nanoparticles. Biomaterials **30,** 919, 2009.
4. Lim, S.M., Oh, S.H., Lee, H.H., Yuk, S.H., Im, G.I., and Lee, J.H. Dual growth factor-releasing nanoparticle/hydrogel system for cartilage tissue engineering. J Mater Sci Mater Med **21,** 2593, 2010.
5. Sundararaj, S.C., Thomas, M.V., Peyyala, R., Dziubla, T.D., and Puleo, D.A. Design of a multiple drug delivery system directed at periodontitis. Biomaterials **34,** 8835, 2013.
6. Shah, N.J., Macdonald, M.L., Beben, Y.M., Padera, R.F., Samuel, R.E., and Hammond, P.T. Tunable dual growth factor delivery from polyelectrolyte multilayer films. Biomaterials **32,** 6183, 2011.
7. Simmons, C.A., Alsberg, E., Hsiong, S., Kim, W.J., and Mooney, D.J. Dual growth factor delivery and controlled scaffold degradation enhance in vivo bone formation by transplanted bone marrow stromal cells. Bone **35,** 562, 2004.
8. Wang, L., Cao, L., Shansky, J., Wang, Z., Mooney, D., and Vandenburgh, H. Minimally invasive approach to the repair of injured skeletal muscle with a shape-memory scaffold. Mol Ther **22,** 1441, 2014.
9. Barnes, G.L., Kostenuik, P.J., Gerstenfeld, L.C., and Einhorn, T.A. Growth factor regulation of fracture repair. J Bone Miner Res **14,** 1805, 1999.
10. Schmid, G.J., Kobayashi, C., Sandell, L.J., and Ornitz, D.M. Fibroblast growth factor expression during skeletal fracture healing in mice. Dev Dyn **238,** 766, 2009.
11. Fei, Y., Gronowicz, G., and Hurley, M.M. Fibroblast growth factor-2, bone homeostasis and fracture repair. Curr Pharm Des **19,** 3354, 2013.
12. Montero, A., Okada, Y., Tomita, M., *et al.* Disruption of the fibroblast growth factor-2 gene results in decreased bone mass and bone formation. J Clin Invest **105,** 1085, 2000.
13. Farhadi, J., Jaquiery, C., Barbero, A., *et al.* Differentiation-dependent up-regulation of BMP-2, TGF-beta1, and VEGF expression by FGF-2 in human bone marrow stromal cells. Plast Reconstr Surg **116,** 1379, 2005.
14. Singhatanadgit, W., Salih, V., and Olsen, I. Up-regulation of bone morphogenetic protein receptor IB by growth factors enhances BMP-2-induced human bone cell functions. J Cell Physiol **209,** 912, 2006.

15. Xiao, L., Ueno, D., Catros, S., *et al.* Fibroblast growth factor-2 isoform (low molecular weight/18 kDa) overexpression in preosteoblast cells promotes bone regeneration in critical size calvarial defects in male mice. Endocrinology **155,** 965, 2014.
16. Gronowicz, G., Hurley, M.M., and Kuhn, L.T. Optimizing BMP-2-induced bone repair with FGF-2. J Am Acad Orthop Surg **22,** 677, 2014.
17. Govender, S., Csimma, C., Genant, H.K., *et al.* Recombinant human bone morphogenetic protein-2 for treatment of open tibial fractures: a prospective, controlled, randomized study of four hundred and fifty patients. J Bone Joint Surg Am **84-A,** 2123, 2002.
18. Swiontkowski, M.F., Aro, H.T., Donell, S., *et al.* Recombinant human bone morphogenetic protein-2 in open tibial fractures. A subgroup analysis of data combined from two prospective randomized studies. J Bone Joint Surg Am **88,** 1258, 2006.
19. Charles, L.F., Woodman, J.L., Ueno, D., Gronowicz, G., Hurley, M.M., and Kuhn, L.T. Effects of low dose FGF-2 and BMP-2 on healing of calvarial defects in old mice. Exp Gerontol **64,** 62, 2015.
20. Jacobs, E.E., Gronowicz, G., Hurley, M.M., and Kuhn, L.T. Biomimetic calcium phosphate/polyelectrolyte multilayer coatings for sequential delivery of multiple biological factors. J Biomed Mater Res A **105,** 1500, 2017.
21. Benkirane-Jessel, N., Lavalle, P., Hubsch, E., *et al.* Short-time tuning of the biological activity of functionalized polyelectrolyte multilayers. Adv Funct Mater **15,** 648, 2005.
22. Decher, G., Hong, J.D., and Schmitt, J. Buildup of ultrathin multilayer films by a self-assembly process: III. Consecutively alternating adsorption of anionic and cationic polyelectrolytes on charged surfaces G Decher JD Hong J Schmitt. Thin Solid Films **210,** 831, 1992.
23. Lvov, Y., Decher, G., Haas, H., Mohwald, H., and Kalachev, A. X-ray analysis of ultrathin polymer films self-assembled onto substrates. Physica B **198,** 89, 1994.
24. Almodovar J., Bacon S., Gogolski J., Kisiday J.D., and Kipper M.J. Polysaccharide-based polyelectrolyte multilayer surface coatings can enhance mesenchymal stem cell response to adsorbed growth factors. Biomacromolecules **11,** 2629, 2010.
25. Facca, S., Cortez, C., Mendoza-Palomares, C., *et al.* Active multilayered capsules for in vivo bone formation. Proc Natl Acad Sci USA **107,** 3406, 2010.
26. Facca, S., Ferrand, A., Mendoza-Palomares, C., *et al.* Bone formation induced by growth factors embedded into the nanostructured particles. J Biomed Nanotechnol **7,** 482, 2011.
27. Macdonald, M.L., Rodriguez, N.M., Shah, N.J., and Hammond, P.T. Characterization of tunable FGF-2 releasing polyelectrolyte multilayers. Biomacromolecules **11,** 2053, 2010.
28. Nadiri, A., Kuchler-Bopp, S., Mjahed, H., *et al.* Cell apoptosis control using BMP4 and noggin embedded in a polyelectrolyte multilayer film. Small **3,** 1577, 2007.
29. Peterson, A.M., Pilz-Allen, C., Kolesnikova, T., Mohwald, H., and Shchukin, D. Growth factor release from polyelectrolyte-coated titanium for implant applications. ACS Appl Mater Interfaces **6,** 1866, 2014.
30. Shah, N.J., Hyder, M.N., Quadir, M.A., *et al.* Adaptive growth factor delivery from a polyelectrolyte coating promotes synergistic bone tissue repair and reconstruction. Proc Natl Acad Sci USA **111,** 12847, 2014.
31. Vodouhe, C., Le Guen, E., Garza, J.M., *et al.* Control of drug accessibility on functional polyelectrolyte multilayer films. Biomaterials **27,** 4149, 2006.
32. Cheng, C.C., Lian, W.S., Hsiao, F.S., *et al.* Isolation and characterization of novel murine epiphysis derived mesenchymal stem cells. PLoS One **7,** e36085, 2012.
33. Mabuchi, Y., Houlihan, D.D., Akazawa, C., Okano, H., and Matsuzaki, Y. Prospective isolation of murine and human bone marrow mesenchymal stem cells based on surface markers. Stem Cells Int **2013,** 507301, 2013.
34. Habibovic P., Barrère, F., van Blitterswijk, C.A., de Groot, K., and Layrolle, P. Biomimetic hydroxyapatite coating on metal implants. J Am Ceram Soc **85,** 517, 2002.
35. Kalajzic, I., Kalajzic, Z., Hurley, M.M., Lichtler, A.C., and Rowe, D.W. Stage specific inhibition of osteoblast lineage differentiation by FGF2 and noggin. J Cell Biochem **88,** 1168, 2003.
36. Jilka, R.L. The relevance of mouse models for investigating age-related bone loss in humans. J Gerontol A Biol Sci Med Sci **68,** 1209, 2013.
37. Cooper, G.M., Mooney, M.P., Gosain, A.K., Campbell, P.G., Losee, J.E., and Huard, J. Testing the critical size in calvarial bone defects: revisiting the concept of a critical-size defect. Plast Reconstr Surg **125,** 1685, 2010.
38. Kuhn, L.T., Liu, Y., Boyd, N.L., *et al.* Developmental-like bone regeneration by human embryonic stem cell-derived mesenchymal cells. Tissue Eng Part A **20,** 365, 2014.
39. Ou, G., Charles, L., Matton, S., *et al.* Fibroblast growth factor-2 stimulates the proliferation of mesenchyme-derived progenitor cells from aging mouse and human bone. J Gerontol A Biol Sci Med Sci **65,** 1051, 2010.
40. Wang, H., Zou, Q., Boerman, O.C., *et al.* Combined delivery of BMP-2 and bFGF from nanostructured colloidal gelatin gels and its effect on bone regeneration in vivo. J Control Release **166,** 172, 2013.
41. Nakamura, Y., Tensho, K., Nakaya, H., Nawata, M., Okabe, T., and Wakitani, S. Low dose fibroblast growth factor-2 (FGF-2) enhances bone morphogenetic protein-2 (BMP-2)-induced ectopic bone formation in mice. Bone **36,** 399, 2005.
42. Springer, I.N., Niehoff, P., Acil, Y., *et al.* BMP-2 and bFGF in an irradiated bone model. J Craniomaxillofac Surg **36,** 210, 2008.
43. Fakhry, A., Ratisoontorn, C., Vedhachalam, C., *et al.* Effects of FGF-2/-9 in calvarial bone cell cultures: differentiation stage-dependent mitogenic effect, inverse regulation of BMP-2 and noggin, and enhancement of osteogenic potential. Bone **36,** 254, 2005.
44. Luong, L.N., Ramaswamy, J., and Kohn, D.H. Effects of osteogenic growth factors on bone marrow stromal cell differentiation in a mineral-based delivery system. Biomaterials **33,** 283, 2012.
45. Maegawa, N., Kawamura, K., Hirose, M., Yajima, H., Takakura, Y., and Ohgushi, H. Enhancement of osteobastic differentiation of mesenchymal stromal cells cultured by selective combination of bone morphogenetic protein-2 (BMP-2) and fibroblast growth factor-2 (FGF-2). J Tissue Eng Regen Med **1,** 306, 2007.
46. Basmanav, F.B., Kose, G.T., and Hasirci, V. Sequential growth factor delivery from complexed microspheres for bone tissue engineering. Biomaterials **29,** 4195, 2008.
47. Kang, M.S., Kim, J.H., Singh, R.K., Jang, J.H., and Kim, H.W. Therapeutic-designed electrospun bone scaffolds: mesoporous bioactive nanocarriers in hollow fiber com-

posites to sequentially deliver dual growth factors. Acta Biomater **16,** 103, 2015.
48. Min, J., Braatz, R.D., and Hammond, P.T. Tunable staged release of therapeutics from layer-by-layer coatings with clay interlayer barrier. Biomaterials **35,** 2507, 2014.
49. Suarez-Gonzalez, D., Lee, J.S., Diggs, A., *et al.* Controlled multiple growth factor delivery from bone tissue engineering scaffolds via designed affinity. Tissue Eng Part A **20,** 2077, 2014.
50. Lei, L., Wang, S., Wu, H., *et al.* Optimization of release pattern of FGF-2 and BMP-2 for osteogenic differentiation of low-population density hMSCs. J Biomed Mater Res A **103,** 252, 2015.
51. Holmes, C., and Stanford, W.L. Concise review: stem cell antigen-1: expression, function, and enigma. Stem Cells **25,** 1339, 2007.
52. Bruder, S.P., Ricalton, N.S., Boynton, R.E., *et al.* Mesenchymal stem cell surface antigen SB-10 corresponds to activated leukocyte cell adhesion molecule and is involved in osteogenic differentiation. J Bone Miner Res **13,** 655, 1998.
53. Lupatov, A.Y., Vdovin, A.S., Vakhrushev, I.V., Poltavtseva, R.A., and Yarygin, K.N. Comparative analysis of the expression of surface markers on fibroblasts and fibroblast-like cells isolated from different human tissues. Bull Exp Biol Med **158,** 537, 2015.

Address correspondence to:
Liisa T. Kuhn, PhD
Department of Biomedical Engineering
University of Connecticut Health Center
263 Farmington Avenue
Farmington, CT 06107

E-mail: lkuhn@uchc.edu

Received: March 7, 2017
Accepted: September 12, 2017
Online Publication Date: November 9, 2017